Contrasting characteristics of aqueous reactive species induced by cross-field and linear-field plasma jets

2017 J. Phys. D: Appl. Phys. 50 245201

(http://iopscience.iop.org/0022-3727/50/24/245201)

IOP Publishing Journal of Physics D: Applied Physics
J. Phys. D: Appl. Phys. **50** (2017) 245201 (7pp) https://doi.org/10.1088/1361-6463/aa7118

Contrasting characteristics of aqueous reactive species induced by cross-field and linear-field plasma jets

Han Xu[1,4], Chen Chen[1,4], Dingxin Liu[1], Dehui Xu[1], Zhijie Liu[1], Xiaohua Wang[1] and Michael G Kong[1,2,3]

[1] State Key Laboratory of Electrical Insulation and Power Equipment, Center for Plasma Biomedicine, Xi'an Jiaotong University, Xi'an 710049, People's Republic of China
[2] Frank Reidy Center for Bioelectrics, Old Dominion University, VA 23508, United States of America
[3] Department of Electrical and Computer Engineering, Old Dominion University, VA 23529, United States of America

E-mail: chenchenxjtuee@sina.cn, liudingxin@mail.xjtu.edu.cn and mglin5g@gmail.com

Received 7 January 2017, revised 1 May 2017
Accepted for publication 4 May 2017
Published 24 May 2017

Abstract

A comparative study on aqueous reactive species in deionized water treated by two types of plasma jets is presented. Classified by the direction of the electric field in the jet device, a linear-field jet and cross-field jet have been set up. Concentrations of several aqueous reactive species are measured quantitatively by chemical fluorescent assays and electron spin resonance spectrometer. Results show that these two-type plasma jets would generate approximately the same gaseous reactive species under the same discharge power, but the linear-field plasma jet is much more efficient at delivering those species to the remote deionized water. This leads to a much more aqueous short-lived species including OH and O_2^- produced in water, which are mainly correlated to the solvation of gaseous short-lived species such as ions and electrons. Regarding the long-lived species of aqueous H_2O_2, the concentration grows faster when treated by the linear-field plasma jet in the initial stage, but after 10 min it is similar to that treated by the cross-field counterpart due to the vapor–liquid equilibrium. The aqueous peroxynitrite is also predicted to be produced as a result of the air inclusion in the feeding gas.

Keywords: atmospheric-pressure plasma jet, linear-field jet, cross-field jet, aqueous reactive species, plasma–liquid interaction

(Some figures may appear in colour only in the online journal)

1. Introduction

Atmospheric-pressure plasma jets have been intensively studied in the last decade due to their great potential in diverse application fields such as surface modification [1, 2] and biomedicine [3, 4]. Excited by electrical power, molecular gas flow is turned into ionized gas which contains various chemical reactive species. During this excitation process, electric field produced by different jet structures can effectively influence the physical and chemical properties of plasma, especially doses of reactive species. Among many types of plasma jet devices [5], most of them can be classified into two types as linear-field and cross-field devices by considering the direction relationship between the electric field and the gas flow field [6]. For linear-field devices, electric field and gas flow field are largely parallel to each other as the common device with just one electrode within a glass tube (the treated substrate in front of the glass tube serves as the other electrode) [5]. But for cross-field devices, these two vector fields are largely perpendicular as those common devices with coaxial electrode structure [5]. Different direction of electric field can directly affect the movement of electrons in plasmas and

[4] The two authors made equal contributions.

therefore influence those electron-related physical and chemical processes, leading to contrasting characteristics of these two types of plasma jets. In particular, the linear-field plasma jet is found to be more efficient at delivering reactive species to the remote substrate under treatment [6–8]. Different jet designs can therefore be used as an effective means to regulate the doses of gaseous reactive species onto the substrate in different applications.

Moreover, in practical applications like cancer therapies [9], wound healing [10], teeth whitening [11], water sterilization [12], etc targets to be treated by plasmas are always covered by liquid layer. Therefore both transportation of gaseous reactive species to aqueous ones and generation of new types of reactive species in liquids happen simultaneously in the interaction between plasmas and liquids. Some of these aqueous reactive species induced by upstream plasmas are shown to have key functions in plasma biomedicine, for example, doses of H_2O_2 and O_2^- are closely related to apoptosis of cancer cells [13]. From previous simulation and experimental work, it is widely accepted that generation and doses of aqueous reactive species are also related to specific characteristics of upstream plasmas. For linear-field and cross-field plasma jets with different electric fields, comparative studies have been reported [6–8, 14, 15]. But a comparative study of the effect that the two configurations have on the liquid substrate has not been thoroughly explored. How much of a difference in reactive species concentration generated in the plasma treated liquid by either the cross field or the linear field plasma jet is an open question. What is the correlation between the characteristics of the two types of gas plasmas and that of their treated liquids? These are all unclear at a fundamental level, and technically a knowledge gap how to regulate doses of aqueous reactive species through tailoring the plasma–liquid interaction to optimize the use of plasmas in many related applications such as biomedicine [16].

In this paper, results from a series of experiments are reported which contrast characteristics of aqueous reactive species induced by the cross-field and linear-field plasma jets. Using chemical fluorescent probes and electron spin resonance (ESR) spectrometry, concentrations of several reactive oxygen species (ROS) induced by two plasms jets have been measured quantitatively to clearly show their differences. In addition, the underlying mechanism is discussed.

2. Experimental methods

The schematic diagrams of two plasma jets are shown in figure 1. Similarly, we use the same quartz tube (4 mm inner and 6 mm outer diameters) and the high-voltage rod electrode located in the axis of the tube (sealed in another smaller quartz tube with a thickness of 0.75 mm) for both linear-field (figure 1(a)) and cross-field (figure 1(b)) plasma jets. The grounded electrodes however are located in a manner to alter the direction of the electric field. Since the delivery of plasma-generated species are mainly through the gas flow, the same direction between electric field and gas flow is thought to strengthen the transportation of charged species into downstream targets. For the linear-field plasma jet, the electric field has a direction from the high-voltage rod electrode to the underneath grounded plate electrode, almost parallel to the gas flow direction. On the contrary, a grounded ring electrode is used which wraps around the outer quartz tube in the cross-field plasma jet, and hence the electric field is mainly in radial direction, perpendicular to the gas flow field. Sinusoidal power supply of $f = 20$ kHz is used to generate plasma. The voltage is measured by using a high-voltage probe (Tektronix, P6015A), and the discharge current is obtained by measuring the voltage drop on the resistance for the linear-field plasma jet, while the current through the grounded ring electrode is also measured by using a current probe (Tektronix, P6021) for the cross-field plasma jet. Two types plasmas are controlled with the same dissipated power of ~127 mW (time-averaged integral of measured voltages and currents) by choosing different peak-to-peak voltages applied on two jet devices (5.6 kV for cross-field jet and 7.6 kV for linear-field jet). In order to investigate whether the changes on jet configurations influence the circuit characteristics, we measure the capacitive currents of two devices by applying a same voltage that is smaller than the breakdown one onto devices to measure the currents in circuit. Since there is no conductive current formed in device before gas breaking down, the currents measured are the capacitive ones representing the capacities of each device. Difference in capacitive current from two devices only reaches 5% in peak value (data not shown).

A glass dish of 2 ml deionized water is located 7 mm away from the jet nozzle. A copper plate electrode under the dish is grounded through a resistance of 100 Ω. The dome tip of the smaller quartz tube has a distance of 3 mm from the jet nozzle (the nozzle of the outer quartz tube), and helium (99.999% purity) flows though the space between the two coaxial quartz tubes with a rate of 3 SLM. Optical emission spectra at the jet nozzles are measured by using a spectrometer (Ocean Optics, USB2000) to distinguish differences in gaseous reactive species in plasmas by two types of jets. Relative position of the fiber to the plasma jet devices is fixed (figure 1). All optical diagnostics and power measurements are done with the water sample in place in order to keep the same circuit characteristics for the whole system.

Chemical fluorescent assays including Amplex® Red reagent (for H_2O_2) and Griess reagent (for NO_2^-/NO_3^-) are used to measure concentrations of aqueous long-lived species in water with both linear and cross field plasma jets [18, 19]. Quantitative concentrations are presented by a microplate reader (Thermo Scientific Varioskan® Flash Reader). At the same time, short-lived species including OH, O_2^- and peroxynitrite (ONOOH and $ONOO^-$) are measured by ESR (BrukerBioSpin GmbH, EMX) [18] using spin traps to capture them into testable spin trap adducts. DMPO (5,5-dimethyl-1-pyrrolineN-oxide, Dojindo, 1 mM) is used to capture OH to generated DMPO-OH and TEMPONE-H (1-hydroxy-2,2,6,6-tetramethyl-4-oxo-piperidine, Enzo, 0.1 mM) is used to capture O_2^- and peroxynitrite to generated TEMPONE.

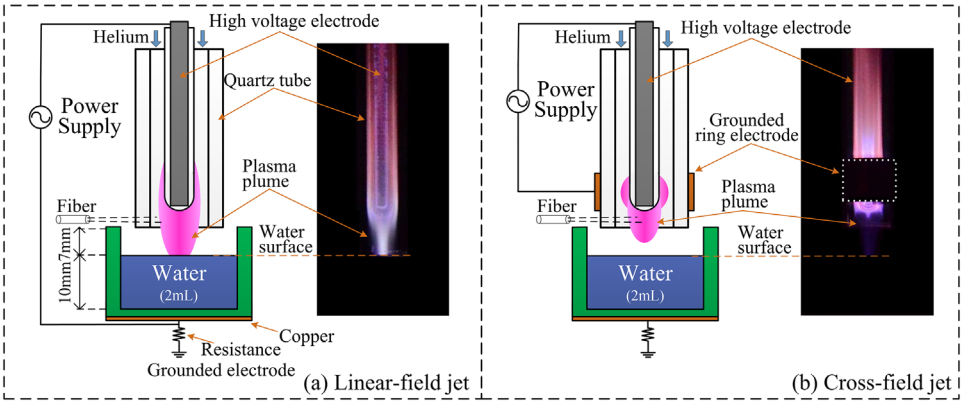

Figure 1. Schematic diagram of two types of plasma jet.

3. Results and discussions

3.1. Generation of gaseous reactive species by two types of plasma jets

Although the discharge power is similar, the plasma plumes for the two jets are very different. Shown in figure 1, the linear-field plasma plume is pronounced and obviously in contact with the water, while the cross-field plasma plume is very weak and just slightly in contact with water downstream. This is in accordance with the literature as the linear-field plasma plume is reported to be longer than cross-field one [6–8, 14, 15]. Enhanced transportation of charged species to the substrate is possible because of the same direction electric field to jet gas flow. It should be emphasized that, the electric charges can move to the remote substrate even though the luminous plasma plume is not in contact with the substrate [17]. For the experimental conditions shown in figure 1, the deposited electric charge per one cycle is measured to be 2.2 nC for the linear-field plasma jet, while it is lower to be 0.87 nC for the cross-field counterpart.

Optical emission spectra present the components of radiative species in gaseous plasma. As shown in figures 2(a) and (b), the emission intensities of OH^*, N_2^{+*}, O^* and He^* are all similar for the two-type plasma jets. For example, the emission intensity of OH(A) at 308.9 nm has a peak value of 1138 a.u. for the linear-field plasma jet, slightly higher than that for the cross-field plasma jet (1025 a.u.). The similarity of emission intensity indicates that two-type plasma jets have similar ability to excite radiative reactive species such as OH(A) though the configuration has changed, suggesting that the *E*/*N* is similar near the nozzle of jet. We also estimate the electric field strength in discharging area for both jets. With the breakdown voltages of 7 kV and 5 kV for linear- and cross-field jet respectively, the E field are estimated as 7×10^5 V m^{-1} and 2×10^6 V m^{-1}. Though higher than linear-jet one, *E* field in cross-field is of perpendicular direction to gas flow. Therefore the normal component of *E* field that points to the liquid surface is less than 2×10^6 V m^{-1}. That is why the generations OH(A) by both jet are not widely different to each other.

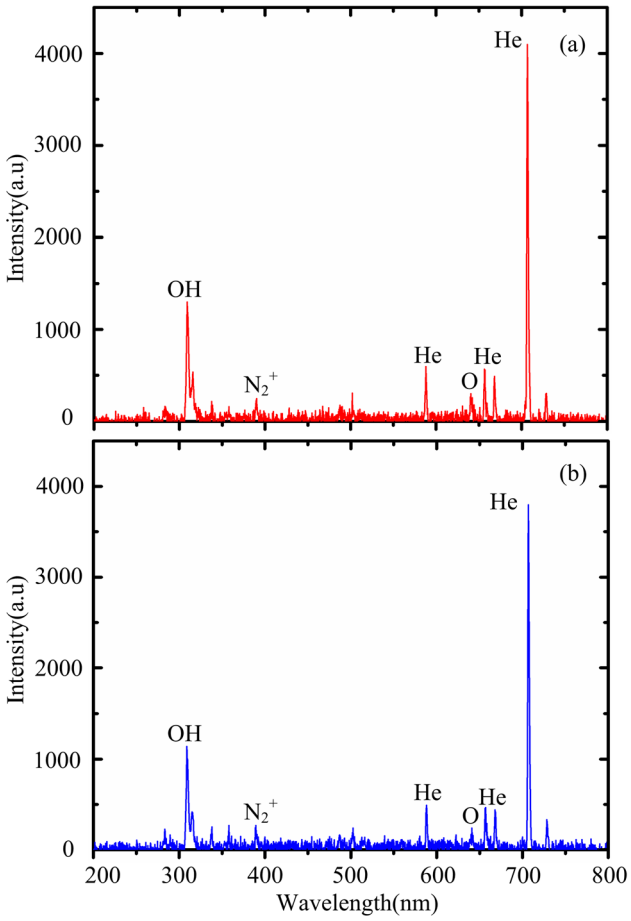

Figure 2. The discharge image and the emission spectra either for the linear-field plasma jet (a) or for the cross-field plasma jet (b).

3.2. Measurements on aqueous reactive species induced by two types of plasma jets with their chemical mechanisms

Aqueous reactive species in deionized water are quite different for the two configurations. Figure 3 shows the quantitative concentration time curves of three tested reactive species. For long-lived species H_2O_2, the Amplex® Red reagent was added into the water right after the plasma treatment to react with H_2O_2. Through a 1:1 reaction in stoichiometry,

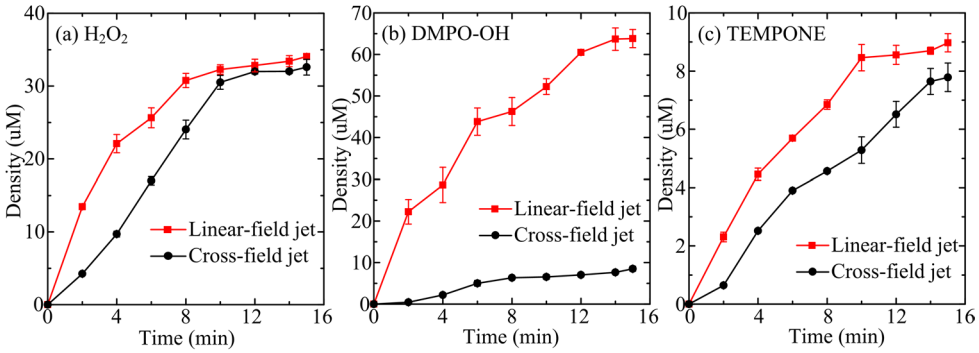

Figure 3. Concentrations of H_2O_2 (a), DMPO-OH (b) and TEMPONE (c) in the deionized water treated by the two-type plasma jets as a function of the treatment time.

the red-fluorescent oxidation product, which was excited at $\lambda = 550$ nm and the emission at $\lambda = 595$ nm can be measured in the microplate reader. Concentration curves of aqueous H_2O_2 induced by the two-type plasmas are shown in figure 3(a). It is clear to see that H_2O_2 concentrations in both cases grow in the first 10 min plasma treatment and then reach closely stable values. Aqueous H_2O_2 induced by linear-field plasma jet grows faster in the first 4 min than cross-field one. According to previous investigations [20, 21], these plasma produced H_2O_2 in liquid can be generated through several chemical pathways. Therefore this observation in figure 3(a) can also be explained by larger particle fluxes of charged species and other short-lived species such as OH on the water. Interestingly, the concentrations of aqueous H_2O_2 induced by the two-type plasma jets are nearly the same (~33 μM) and invariable after 10–15 min of plasma treatment. A possible explanation of this phenomenon is that the H_2O_2 reaches vapor–liquid equilibrium for both plasma jets when the treatment time is larger than 10 min [22]. H_2O_2 can be generated in gaseous phase because of the reaction between plasma and water vapor near surface and penetrate into aqueous phase through absorption [22], or be generated directly in liquid through aqueous chemical network [20]. With 10 min plasma treatment, total H_2O_2 in liquid reach equilibrium with the H_2O_2 outside, leading to a stable concentration in water. This also implies that the yields of gaseous H_2O_2 by the two-type plasma jets are similar despite of their different electrode structures. In this case their gaseous densities can be evaluated as ~8.3×10^{15} m^{-3} based on Henry's Law [23]. Also, the Griess reagent was used to detect NO_2^- and NO_3^-, and the absorbance was measured at $\lambda = 550$ nm. However, no detectable signal was detected, indicating that the concentration of NO_2^-/NO_3^- is lower than the detection limit of ~1 μM.

The concentrations of short-lived aqueous species were measured by ESR spectrometer. Instead of short-lived and untestable species themselves, concentrations of spin adducts that with longer lifetime could be obtained from the ESR spectra, calibrated by using a stable radical, TEMPO. Although the trapping reagents have been frequently reported for the measurement of OH and/or O_2^-, it should be noted that they might also react with other reactive species to produce the same spin adducts. For example, TEMPONE-H can react with peroxynitrite with a large rate coefficient of 6×10^9 M^{-1} s^{-1}, and produce TEMPONE as well [24]. Therefore, the concentrations obtained by ESR might not only reflect concentrations of O_2^-, but also some other species such as peroxynitrite. The concentration curves of spin trap adduct obtained by ESR measurement for DMPO-OH and TEMPONE are shown in figures 3(b) and (c). Further discussion will be made on the correlation of short-lived species to their spin adducts below.

As shown in figure 3(b), concentrations of DMPO-OH from two types of plasma jets increase with the plasma treatment time. Comparatively the one for the linear-field plasma jet is larger by 7.5–13.1 fold. DMPO can react with both OH and O_2^- to produce DMPO-OH, but the reaction with OH is much faster, and hence the DMPO will bind quicker with OH in presence of the same amount of OH and O_2^- [25]. Furthermore, the amount of O_2^- should be much lower than that of OH by comparing the concentrations of DMPO-OH and TEMPONE as shown figures 3(b) and (c). Based on these facts, results of DMPO-OH should mainly consist of the trapped OH radicals. Therefore, it can be concluded the linear-field plasma jet is much more efficient to produce aqueous OH compared to the cross-field counterpart. According to recent simulation results reported by our group and others [18–21], three physicochemical pathways are important for the production of aqueous OH during the plasma treatment, including the solvation of gaseous OH, the VUV photo-dissociation of H_2O at the gas–liquid interface, and the reactions in water as given by:

$$O_3^- + H^+ \rightarrow O_2 + OH \quad \text{(R1)}$$

$$H_2O^+ + H_2O \rightarrow H_3O^+ + OH \quad \text{(R2)}$$

$$H_3O^+ + OH^- \rightarrow H_2O + H + OH. \quad \text{(R3)}$$

Compared to the cross-field plasma jet, the linear-field plasma jet can be in contact with the water (see figure 1) and hence more short-lived species, especially charged species, VUV photons and free radicals such as OH, can dissolve into the water, which will enhance all these three pathways as presented above. This is why the linear-field plasma jet is more pronounced for the production of aqueous OH in water. What should also be noticed is that, results from ESR spectrometer are the concentrations of DMPO-OH, spin trap adducts from reaction between DMPO and OH, not OH themselves. With

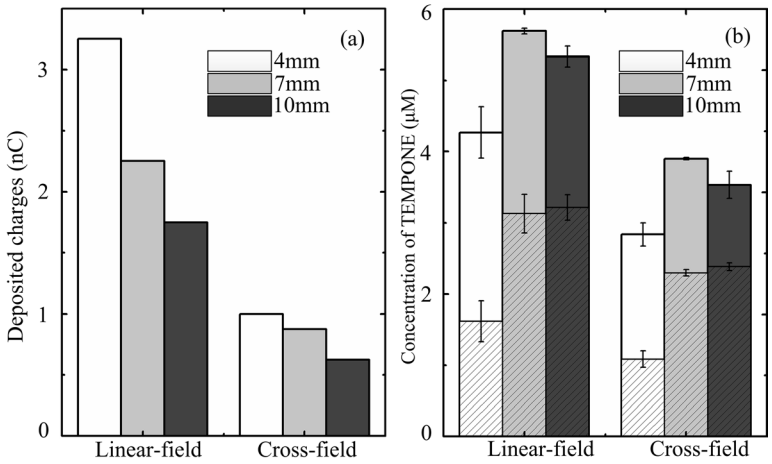

Figure 4. The amounts of deposited charge per voltage-cycle (a) and the concentrations of TEMPONE (b) after 6 min treatment by the two-type plasma jets for different gap distances of 4, 7 and 10 mm. The bars with diagonal lines in (b) represent the values after using SOD.

a high reaction rate constant and high concentration in order to fully capture OH, DMPO keep reacting with OH at the moment OH being generated. Therefore the process of capturing becomes a process of accumulating all generated OH in liquid. If the spin traps are not added in water, most generated OH will be rapidly consumed by other components in water because their high reactivity. Consequently, concentrations of DMPO-OH are reflecting the total generation of OH during plasma treatment [25]. That is why the concentrations of DMPO-OH can be as high as 60uM, even higher than long-lived species H_2O_2.

As shown in figure 3(c), the concentration of TEMPONE for the linear-field plasma jet increases fast in the first 10 min of plasma treatment, but changes only a little in the following treatment process. On the contrary, case of cross-field plasma jet continues to increase during the entire process of plasma treatment, and comparatively it is lower by 1.8–3.5 μM when the plasma treatment time is larger than 2 min. This difference is most pronounced at the plasma treatment time of 2 min, since it corresponds to 3.6 fold in quantity, but it only corresponds to 1.1 fold at the instant of 15 min. As discussed above, the measured TEMPONE should mainly consist of the trapped O_2^- and peroxynitrite, and hence it can be concluded that the total concentration of aqueous O_2^- and peroxinitrite is larger in the water treated by the linear-field plasma jet. Based on our previous study [20], the main production pathway of the aqueous O_2^- is the electron attachment by the dissolved oxygen:

$$e + O_2 \rightarrow O_2^-. \quad \text{(R4)}$$

While the aqueous peroxynitrite was reported to be mainly produced by the solvation of gaseous ONOOH and the aqueous reaction between NO and HO_2 [21]:

$$NO + HO_2 \rightarrow ONOOH. \quad \text{(R5)}$$

The gaseous ONOOH is produced when the plasma plume meets N_2 or other nitrogen-containing molecules in surrounding air outside the jet nozzle, and so does the gaseous NO. The solvation of gaseous NO is then attributed for the production of aqueous ONOOH in water via (R5). According to (R4) and (R5), the electron flux onto water surface is mainly responsible for the production of O_2^-, while the air additive in helium is mainly responsible for the production of peroxynitrite. This gave us an inspiration to clarify the amounts of O_2^- and peroxynitrite as precursors for TEMPONE by varying the electron flux and the air additions.

3.3. Tests on the chemical mechanisms of generation of aqueous reactive species

In order to investigate the generation mechanisms of tested aqueous reactive species we mentioned above, we varied the gap width between the jet nozzle and the water surface from 4 mm to 10 mm to change the admixture of air into plasma plume, while keeping the discharge power constant to be ~127 mW and the treatment time of 6 min. As shown in figure 4(a), charges deposited on the water during a voltage cycle decrease with the gap width for the two-type plasma jets, because more voltage is needed to sustain the discharge and hence the current (mainly corresponding to the electron flux) is reduced. The concentrations of TEMPONE for the two-type plasma jets are shown in figure 4(b) (the entire bars), which increase first and then slightly decrease. The trend is different to that of the deposited charge. However, if a scavenger of O_2^-, superoxide dismutase from bovine erythrocytes (SOD, sigma, USA)), is added into the water together with the TEMPONE-H, the residual TEMPONE has its concentration increasing with the gap width (see the bars with diagonal lines in figure 4(b)). It should be noted that the used amount of SOD was large enough, i.e. the concentration of TEMPONE does not decrease anymore with the increase amount of SOD. As discussed above, the residual TEMPONE is most possible to consist of the trapped peroxynitrite, and the increase of its concentration with the gap width can be explained by the more air additive with the expansion of the plasma plume. Considering the hydrophobic characteristics of NO with low Henry's constant, aqueous peroxynitrite might mostly be generated through solvation of gasesous ONOOH. Moreover, the different value between the TEMPONE concentrations with and without the use of SOD should represents the concentration

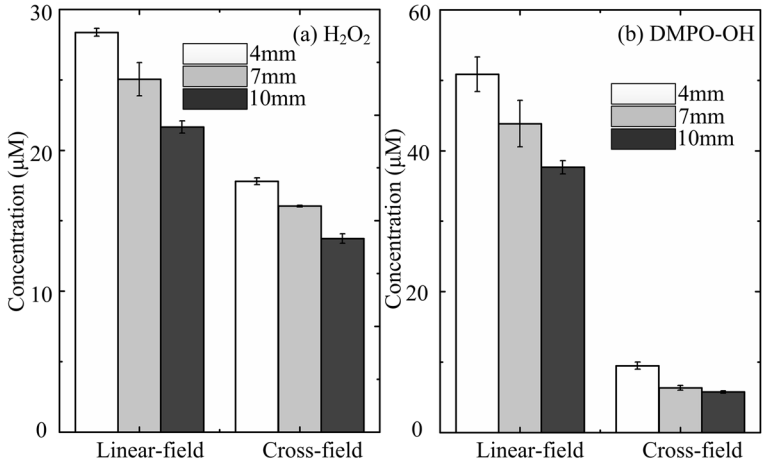

Figure 5. The concentrations of H_2O_2 (a) and DMPO-OH (b) after 6 min treatment by the linear-field and cross-field plasma jets for different gap distances of 4, 7 and 10 mm.

of trapped O_2^-, which decreases with the incresing gap distance, similar to the trend of the deposited charge as shown in figure 4(a). Quantitatively, the deposited charges for the linear-field plasma jets are larger than the cross-field counterparts by 2.5–3.5 fold for the three gap distances, while the concentrations of trapped O_2^- are 1.5–3.5 fold. This implies that the electron attachment by the dissolved oxygen (R4) plays a significant role for the aqueous O_2^- production.

The dependence of the concentrations of H_2O_2 and DMPO-OH on the gap distance is shown in figure 5, from which it can be seen that the concentrations keep decreasing with the increasing discharge gap distance. The reductions of H_2O_2 concentrations are ~23% for both types of plasma jets, while for DMPO-OH concentrations the reductions are 30% and 45% for the linear-field jet and cross-field jet, respectively. The concentration of DMPO-OH largely represents the generation of OH radicals as discussed above. For the linear-field plasma jet, the reduction of aqueous OH should be mainly ascribed to the density decrease of the related plasma species (gaseous OH, VUV photons, etc) due to the extension of plasma plume. In comparison, for the cross-field plasma jet the reduction is also ascribed to the short lifetimes of the related plasma species, and the amounts of such species moving into the water would decrease sharply with the increasing gap distance. This is why the reduction of the DMPO-OH concentration is more pronounced for the cross-field plasma jet. On the contrary, H_2O_2 have very long lifetime and hence their reduction degrees are similar for the two-type plasma jets.

4. Conclusion

In conclusion, the linear-field and cross-field plasma jets were comparatively studied in this letter. It is found that with very little influence on circuit structure, two-type plasma jets with change in configuration have similar efficient to produce gaseous reactive species such as OH(A) and H_2O_2, but the linear-field plasma jet is much more efficient to deliver those species to the remote deionized water under treatment. In comparison, the concentration of aqueous H_2O_2 induced by the linear-field plasma jet grows faster in the initial stage of treatment, but after 10 min it is similar to that induced by the cross-field counterpart due to the vapor–liquid equilibrium. The concentration of aqueous OH induced by the linear-field plasma jet is 7.5–13.1 fold larger, and for the aqueous O_2^- it is 1.5–3.5 fold larger for our experimental conditions. These two short-lived species are mainly produced directly and/or indirectly by the solvation of the gaseous short-lived species. In particular, it is found that dose of the dissolved electrons shows relations with generation of H_2O_2 and O_2^- in solution, which agreed with the chemical pathways of electron attachment reaction with oxygen from simulations. Moreover, the aqueous peroxynitrite is indirectly evidenced to exist which is due to the air inclusion in the feeding gas.

Acknowledgement

This work was supported by the National Science Foundation of China (Grant No. 51677147 and 51521065), the Fundamental Research Funds for the Central Universities and the State Key Laboratory of Electrical Insulation and Power Equipment (Grant No. EIPE14123 and No. EIPE17309).

References

[1] Liston E M, Martinu L and Wertheimer M R 1993 Plasma surface modification of polymers for improved adhesion: a critical review *J. Adhes. Sci. Technol.* **7** 1091
[2] Shao T, Zhang C, Long K H, Zhang D D, Wang J, Yan P and Zhou Y 2010 Surface modification of polyimide films using unipolar nanosecond-pulse DBD in atmospheric air *Appl. Surf. Sci.* **256** 3888
[3] Kong M G, Kroesen G, Morfill G, Nosenko T, Shimizu T, van Dijk J and Zimmermann J L 2009 Plasma medicine: an introductory review *New J. Phys.* **11** 115012
[4] Xu D H, Liu D X, Wang B Q, Chen C, Chen Z Y, Li D, Yang Y J, Chen H L and Kong M G 2015 *In situ* OH generation from and H_2O_2 plays a critical role in plasma-induced cell death *Plos One* **6** e0128205
[5] Lu X, Naidis G V, Laroussi M, Reuter S, Graves D B and Ostrikov K 2016 Reactive species in non-equilibrium

atmospheric-pressure plasmas: generation, transport, and biological effects *Phys. Rep.* **630** 184
[6] Walsh J L and Kong M G 2008 Contrasting characteristics of linear-field and cross-field atmospheric plasma jets *Appl. Phys. Lett.* **93** 111501
[7] O'Connor N and Daniels S 2011 Passive acoustic diagnostics of an atmospheric pressure linear field jet including analysis in the time-frequency domain *J. Appl. Phys.* **110** 013308
[8] Gaens W V, Bruggeman P J and Bogaerts A 2014 Numerical analysis of the NO and O generation mechanism in a needle-type plasma jet *New J. Phys.* **16** 063054
[9] Vandamme M *et al* 2012 ROS implication in a new antitumor strategy based on non-thermal plasma *Int. J. Cancer* **130** 2185–94
[10] Isbary G *et al* 2012 Successful and safe use of 2 min cold atmospheric argon plasma in chronic wounds: results of a randomized controlled trial *Br. J. Dermatol.* **167** 404–10
[11] Sun P *et al* 2010 Tooth whitening with hydrogen peroxide assisted by a direct-current cold atmospheric-pressure air plasma microjet *IEEE Trans. Plasma Sci.* **38** 1892–96
[12] Malik M A, Ghaffar A and Malik S A 2001 Water purification by electrical discharges *Plasma Sources Sci. Technol.* **10** 82
[13] Mates J M and Sanchez-Jimenez F M 2000 Role of reactive oxygen species in apoptosis: implications for cancer therapy *Int. J. Biochem. Cell* B **32** 157–70
[14] Cao Z, Walsh J L and Kong M G 2009 Atmospheric plasma jet array in parallel electric and gas flow fields for three-dimensional surface treatment *Appl. Phys. Lett.* **94** 021501
[15] Hofmann S, van Gils K, van der Linden S, Iseni S and Bruggeman P 2014 Time and spatial resolved optical and electrical characteristics of continuous and time modulated RF plasmas in contact with conductive and dielectric substrates *Eur. Phys. J.* D **68** 40430
[16] Bruggeman P J *et al* 2016 Plasma–liquid interactions: a review and roadmap *Plasma Sources Sci. Technol.* **25** 053002
[17] Norberg S A, Tian W, Johnsen E and Kushner M J 2014 Atmospheric pressure plasma jets interacting with liquid covered tissue: touching and not-touching the liquid *J. Phys. D: Appl. Phys.* **47** 475203
[18] Liu D X, Liu Z C, Chen C, Yang A J, Li D, Rong M Z, Chen H L and Kong M G 2016 Aqueous reactive species induced by a surface air discharge: heterogeneous mass transfer and liquid chemistry pathways *Sci. Rep.* **6** 23737
[19] Liu Z C, Liu D X, Chen C, Li D, Yang A J, Rong M Z, Chen H L and Kong M G 2015 Physicochemical processes in the indirect interaction between surface air plasma and deionized water *J. Phys. D: Appl. Phys.* **48** 495201
[20] Chen C, Liu D X, Liu Z C, Yang A J, Chen H L, Shama G and Kong M G 2014 A model of plasma-biofilm and plasma-tissue interactions at ambient pressure *Plasma Chem. Plasma Process.* **34** 403
[21] Tian W and Kushner M J 2014 Atmospheric pressure dielectric barrier discharge interacting with liquid covered tissue *J. Phys. D: Appl. Phys.* **47** 165201
[22] Winter J *et al* 2014 Tracking plasma generated H_2O_2 from gas into liquid phase and revealing its dominant impact on human skin cells *J. Phys. D: Appl. Phys.* **47** 285401
[23] Zhou X L and Lee Y N 1992 Aqueous solubility and reaction kinetics of hydroxymethyl hydroperoxide *J. Phys. Chem.* **96** 265
[24] Dikalov S, Skatchkov M and Bassenge E 1997 Quantification of peroxynitrite, superoxide, and peroxyl radicals by a new spin trap hydroxylamine 1-hydroxy-2,2,6,6-tetramethyl-4-oxo-piperidine *Biochem. Bioph. Res. Commum.* **230** 54–57
[25] Tresp H, Hammer M U, Weltmann K-D and Reuter S 2013 Quantitative detection of plasma-generated free radicals in liquids by electron paramagnetic resonance spectroscopy *J. Phys. D: Appl. Phys.* **46** 435401